Cross-Conjugated n-Dopable Aromatic Polyketone

Voortman, Thomas P.; Bartesaghi, Davide; Koster, L. Jan Anton; Chiechi, Ryan C.

Published in:
Macromolecules

DOI:
10.1021/acs.macromol.5b01387

Publication date:
2015

A Cross-conjugated n-Dopable Aromatic Polyketone

Thomas P. Voortman,[†,‡] Davide Bartesaghi,[‡,¶] L. Jan Anton Koster,[‡] and Ryan C. Chiechi[*,†,‡]

†Stratingh Institute for Chemistry, University of Groningen, Nijenborgh 4, 9747 AG Groningen, the Netherlands

‡Zernike Institute for Advanced Materials, University of Groningen, Nijenborgh 4, 9747 AG Groningen, the Netherlands

¶Dutch Polymer Institute, P. O. Box 902, 5600AX, Eindhoven, the Netherlands

E-mail: r.c.chiechi@rug.nl

Abstract

This paper describes the synthesis and characterization of a high molecular weight cross-conjugated polyketone synthesized *via* scalable Friedel-Crafts chemistry. Cross-conjugated polyketones are precursors to conjugated polyions; they become orders of magnitude more conductive after a two-electron reduction and demonstrate reversible spinless doping upon protonation with acids. Cross-conjugated polyketones are a new polymer platform that posses the same optoelectronic tunability as conventional polymers but with excellent thermal- and oxidative stability. We constructed a proof-of-concept organic light-emitting diode device and demonstrate that a cross-conjugated polyketone can be successfully used as an n-dopable semiconducting material.

Introduction

Conjugated polymers are conceived as candidates for mass production of thin, mechanically compliant devices *via* roll-to-roll (R2R) processing with a lower carbon footprint than their brittle silicon-based counterparts.[1] However, full scale production of optoelectronic devices can, arguably, only be achieved by processing from environmentally benign solvents such as water or ethanol[2,3] which, unfortunately, are poor solvents for conventional conjugated polymers. In recent years much progress towards "green"-processable[4] conjugated polymers has been made utilizing two main strategies: (1) functionalization with ionic pendant groups, and (2) installing polar solubilizing groups.[5] Oft-used polar solubilizing groups are ethylene oxides, offering good solubility in most organic solvents, including polar solvents such as ethyl acetate and alcohols.[6] Conjugated polyelectrolytes (CPEs) use ionic pendant groups to achieve water-solubility; however, CPEs are amphiphilic (*i.e.*, they comprise hydrophilic and hydrophobic character), causing deleterious aggregation and precipitation, resulting in poor film quality.[7] Söndergaard *et al.*, took a different strategy based on polythiophene with thermally cleavable water-soluble pendant groups and demonstrated a proof-of-concept organic photovoltaic (OPV) device processed solely from water.[3]

We are taking an alternative chemistry approach to this problem by synthesizing a semi-conducting polymer that is not only intrinsically water-soluble but also completely water-processable. Conjugated polyions (CPIs) are a new class of robust, semi-conducting polymers in which charges reside inside the conjugated main chain, either transiently or permanently. Earlier, we demonstrated an n-dopable ketone containing cross-conjugated polymer **PTK** (Scheme 1) which, when reduced, becomes linearly conjugated by the inclusion of charges and becomes orders of magnitude more conductive. However, these charges are transient and exist only under a negative bias or under strongly acidic conditions.[8] The general route towards intrinsic CPIs is to render a cross-conjugated polyketone fully conjugated by the addition of nucleophiles *via* "spinless doping" in a post-polymerization modification.[9] This process extends the conjugation of the polymer and imparts cationic character, allowing

water to solvate the backbone.[7]

Thus, cross-conjugated polyketones are precursors to CPIs that are highly charged, pristine semiconductors; they are charged but do not contain spin. Incorporating cross-conjugated units in conjugated polymers is a known strategy to improve air stability of doped semiconducting polymers.[10,11] In fused ring systems, despite reduced delocalization of charge carriers along the polymer backbones of such materials, high field mobilities (0.08–0.15 $cm^2\ V^{-1}\ s^{-1}$) can be achieved due to high π-π stacking.[12–16] The number of cross-conjugated ketone containing polymers reported in the literature, however, is limited to only a few examples, two of which, **PTK**[8] and **PFK**[9] (Scheme 1), were reported by us. To the best of our knowledge, the only other cross-conjugated polyketones were reported by Hudson and Stevens and Curtis and coworkers. They synthesized their cross-conjugated aromatic polyketones *via* an Aldol condensation of cyclic ketones with aromatic dialdehydes[17] and by copolymerization of bis(chloromercuri)thiophenes with CO in hot pyridine with a Pd catalyst under 500 psi of CO,[18,19] respectively. However, the materials form Hudson and Stevens suffered from low solubility (they were partially cross-linked) and incomplete dehydration led to the inclusion of alcohol groups in the main chain. The poly(thienylene ketone)s from Curtis and coworkers had good solubility and moderate degrees of polymerization (P_n) (9-15 repeat units) but were not reversibly n-dopable. We synthesize cross-conjugated polyketones by Friedel-Crafts (F-C) acylation polycondensation which was initially employed to produce poly(ether ketone) (PEK) on pilot scale.[20,21] Poly(aryl ether ketones) (PAEKs) are well known for their high thermal stability, good solvent resistance, and good mechanical properties, however, they are not conjugated (or semiconducting).[22–25]

The optical band gap (E_g^{opt}) of conjugated polymers typically saturate already at low P_n,[26,27] the excellent physical properties associated with commodity plastics (such as mechanical compliance and durability), however, are significantly affected by molecular weight.[28,29] Unfortunately, despite numerous optimizations of the polycondensation reaction to synthesize CPIs based on **PFK**, molecular weights remained relatively low ($P_n \sim 9$).[9] To address

this shortcoming, we set out to optimize the polymerization conditions in order to synthesize higher molecular weight cross-conjugated aromatic polyketones with potentially interesting optoelectronic properties. The F-C acylation reaction is sensitive to nucleophile strength; therefore, increasing the donor character of the monomer should improve reactivity towards F-C acylation polycondensation, and result in a higher molecular weight polymer. This paper describes the synthesis and full characterization of a high molecular weight and high thermally stable ketone-containing conjugated polymer, poly[((thiophen-2-yl)fluorene(thiophen-2-yl))-*alt*-(1,4-phenylene)di-methanone] (**PTFK**, Scheme 1), synthesized *via* F-C chemistry. To test the application of a cross-conjugated, ketone-containing polymer as a durable, n-dopable optoelectronic material, we additionally constructed a proof-of-concept organic light-emitting diode (OLED). To prove that **PTFK** can serve as a precursor to a CPI, we converted it to a CPI both by treatment with acid and a strong alkylating agent.

Results and Discussion

Synthesis and Characterization

The F-C polycondensation method is a straightforward route towards ketone containing polymers that benefits over Stille or Suzuki-Miyaura coupling reactions in that it does not require transition-metal catalysts, which greatly improves the scalability of the reaction. Commonly used solvents that are inert towards F-C acylation conditions include 1,2-dichloromethane (DCM), 1,2-dichloroethane (DCE), carbon disulfide (CS_2), and nitromethane (CH_3NO_2).[30] We have demonstrated that a successful polycondensation can be performed in DCM to afford **PFK**, however, the kinetics of polymerization seemed to be limited by the low boiling temperature and/or solubility of the product in DCM, resulting in low P_n.[9] We also performed the polycondensation reaction in DCE, however, this resulted in an intractable, black tar. It is intuitive that conjugated polymers—usually consisting of rigid backbones—benefit from solvents that keep the propagating chains solubilized longer at elevated reaction

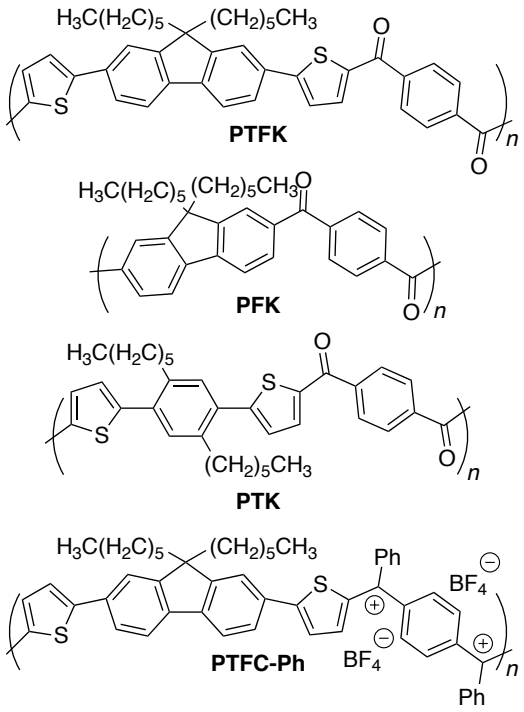

Scheme 1: Structures of the cross-conjugated ketones **PTFK**, **PFK**, and **PTK**, and the permanent CPI **PTFC-Ph** obtained from **PTFK** as discussed in the main text.

temperatures. However, the list of alternative solvents is limited and aromatic solvents, in general, cannot be used as they are reactive towards F-C acylation. The use of 1,3,5-trichlorobenenzene (TCB) was proposed in a patent in 1987[31] and we were able to use it to polymerize **PFK**.[9] We observed a dramatic improvement in molecular weight, but the polymer had a bimodal molecular-weight distribution. Furthermore, because TCB is a solid at room temperature, it needs to be removed from the product by distillation. Due to sublimation at reduced pressures and low polymer yields, we eventually abandoned this route. Although chlorobenzene readily reacts under F-C acylation conditions, *ortho*-dichlorobenzene (ODCB) is remarkably stable and can even be separated from its isomers by reacting the mixture with strong Lewis Acids.[25] Gay and Brunette reported that ODCB can indeed be used as a F-C solvent with a large excess of $AlCl_3$.[32] However, reacting 9,9-dihexylfluorene and terephthaloyl chloride with $AlCl_3$ at elevated temperatures in ODCB did not result in an increase in P_n of **PFK**. This is clearly a problem of thermodynamics; fluorene is too deacti-

vating for an efficient acylation polycondensation. To address this problem, we installed two thiophene units adjacent to the fluorene to increase the electron-donating character, which should increase its reactivity and, therefore, P_n.

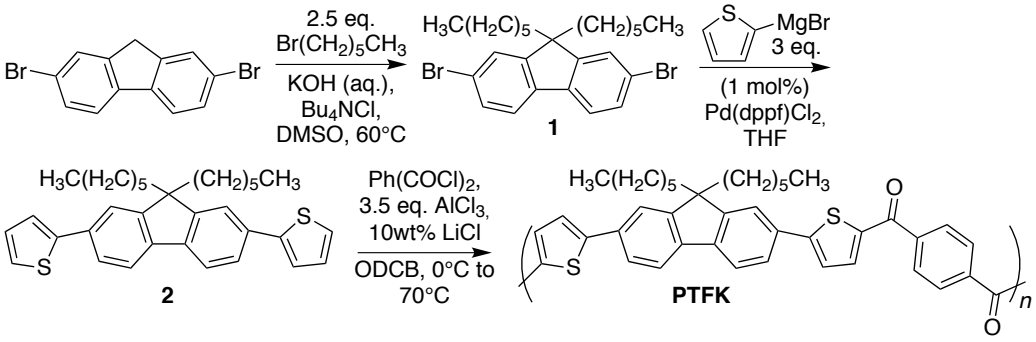

Scheme 2: Synthetic route towards **PTFK**.

We synthesized **PTFK** and the corresponding monomer **2** according to Scheme 2 as described in the experimental section (see Fig. S1 & Fig. S2 for ^{1}H NMR spectra). The F-C polycondensation reaction requires anhydrous conditions, thus, we distill ODCB over CaH_2 just before each polymerization. Furthermore, we carefully purified and dried both monomers and stored them *in vacuo* until use. We chose a polymerization temperature of 70 – 75 °C for 18-20h because at higher temperatures the polymerization yielded mostly insoluble material. In fact, under these conditions approximately 10-20 wt% of the polymer is consistently insoluble, suggesting that we reach the solubility limit of the polymer in common organic solvents.

Thanks to the straightforward synthesis and purification of monomer **2** and the ubiquity of terephthaloyl chloride in plastics, we were able to obtain multiple grams of high molecular weight **PTFK** with $P_n \sim 14$ at peak-average molecular weight ($\bar{M}_p$) and $P_n \sim 62$ at weight-average molecular weight ($\bar{M}_w$) (Fig. S5). **PTFK** is soluble in common organic solvents at high enough concentrations to be able to obtain free-standing films easily. Characterization of the polymer by ^{1}H NMR (Fig. 1 & Fig. S2) revealed extra peaks (and minor butylated hydroxytoluene and "H grease" impurities) that probably correspond to polymer end-groups and are highlighted by asterisks (Fig. 1). It is unlikely that these peaks are from left-over

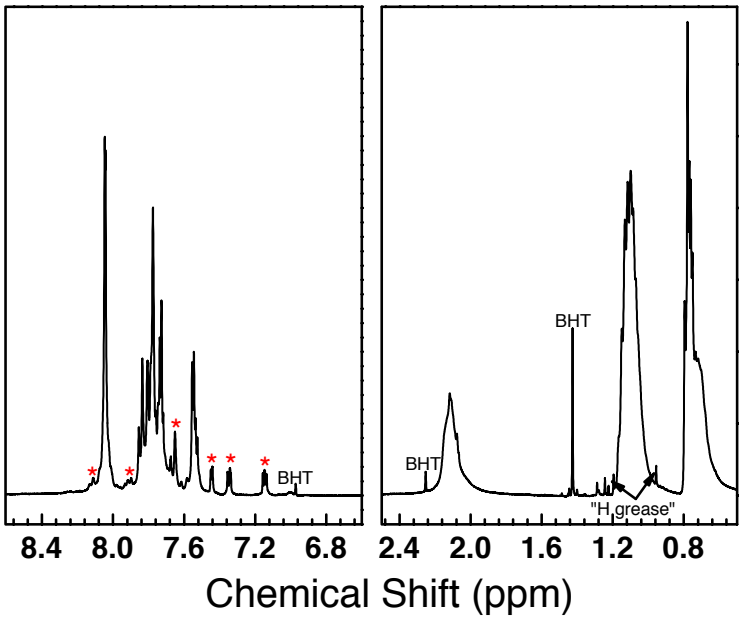

Figure 1: ^{1}H NMR spectrum of **PTFK** in CD_2Cl_2 in which the peaks corresponding to polymer end-groups are indicated by an asterisk. Despite extensive purification some minor impurities could not be completely removed.

monomeric material, considering the excellent solubility of **2** in acetone (which was used during soxhlet extraction). *Via* end-group analysis we find P_n ~ 15 and number-average molecular weight ($\bar{M}_n$) ~ 10,500 which is in excellent agreement with gel permeation chromatography (GPC) data (see Supporting Information). The inclusion of carbonyl units into the polymer is further confirmed by ^{13}C NMR and FT-IR (Fig. S3 and Fig. S4, respectively).

We characterized **PTFK** further by thermogravimetric analysis (TGA) and differential scanning calorimetry (DSC) to elucidate the thermal properties of the polymer. The results are shown in Fig. 2. **PTFK** exhibits a glass transition temperature (T_g) at 144 °C with no other visible thermal transitions, as is common for conjugated polymers. The T_g roughly scales with molecular weight (up to a certain threshold value). Assuming similar conformational freedom, the considerably higher T_g of **PTFK** compared to **PFK** (T_g ~ 97 °C) clearly demonstrates the effect of the higher molecular weight on the thermal properties of these polyketones.[33] Despite careful drying *in vacuo* at temperatures up to 100 °C the baseline of the decomposition curve of **PTFK** is slightly skewed until 310 °C and 5% weight

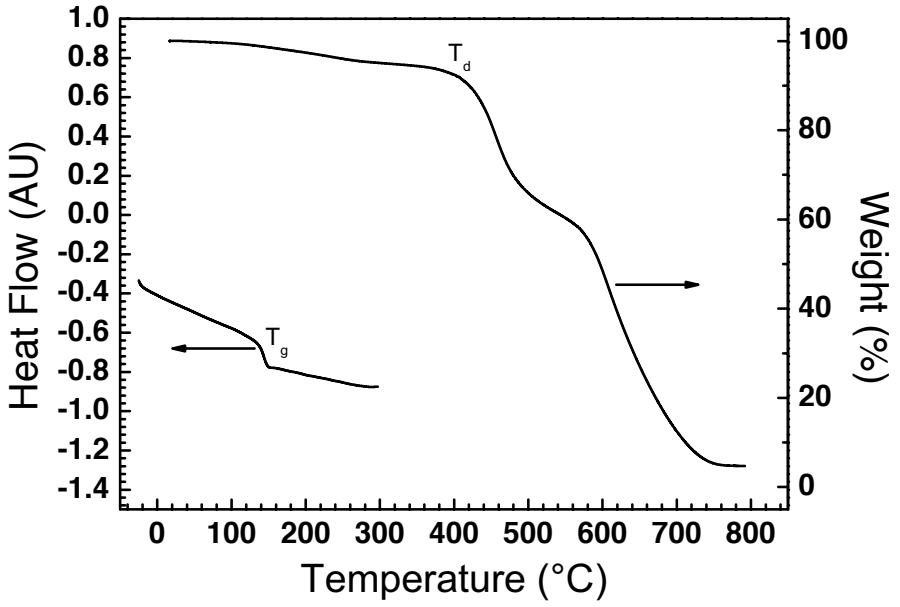

Figure 2: Thermogravimetric analysis (TGA) and differential scanning calorimetry (DSC) plots of **PTFK** showing typical glassy behavior with T_g at 144 °C and T_d at 400 °C.

loss, indicating expulsion of some volatiles. The polymer has a clear thermal decomposition temperature (T_d) at 400 °C, which is similar to that of **PFK** (420 °C), and at 495 °C a second decomposition step is visible. The first decomposition step totals 25wt% and likely corresponds to the loss of the hexyl pendant groups (*i.e.*, ~ 27wt%). At temperatures above 495 °C the rest of the polymer decomposes completely.

Optoelectronic Characterization

With high molecular weight and thermally stable **PTFK** in hand, we set out to elucidate its optoelectronic properties. First, we acquired absorption and emission spectra of **PTFK** in solution, which are shown in Fig. 3. The inclusion of thiophene units in **PTFK** results in an absorption that is red-shifted by 75 nm relatively to **PFK** to λ_{max}^{abs} ~ 415 nm with a band edge at ~ 470 nm. This bathochromic shift is attributed to the significantly larger cross-conjugated chromophore in **PTFK** compared to the smaller chromophore in **PFK**, leading to a smaller optical band gap (E_g^{opt}) of 2.6 eV (vs. 3.3 eV for **PFK**). Interestingly, the large Stokes shift of 175 nm that we observed for **PFK** is considerably smaller (by 80 nm) for **PTFK**, which

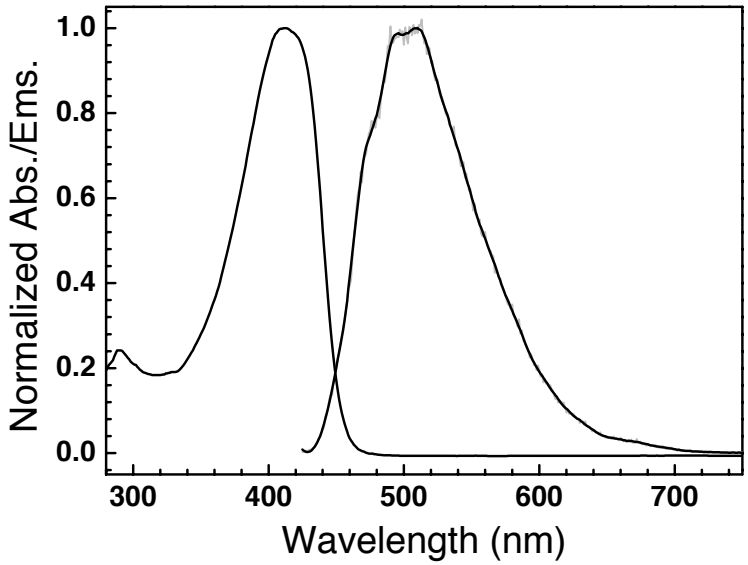

Figure 3: Normalized absorption and emission (smoothed for clarity) spectra of **PTFK** measured in CH_2Cl_2 with $\lambda_{max}^{abs} \sim 415$ nm and $\lambda_{max}^{ems} \sim 510$ nm, respectively.

emits at 510 nm. The fact that the bathochromic shift in absorption is not paired with an equal shift in emission indicates that, either **PTFK** emits from a different state than **PFK** or that that the thiophene units introduce significant conformational flexibility.

The effective conjugation length of CPIs can be tuned post-polymerization by modulating the number of charges in the conjugated backbone. Likewise, **PTFK** can be chemically "doped" by treatment with strong acids. Solutions of **PTFK** acidified with H_2SO_4 are deep blue and revert back to yellow when neutralized. Protonation of the carbonyl units breaks the cross-conjugation and, as carbocations are formed inside the conjugated backbone, the conjugation is extended, leading to a decrease in the band gap from 2.6 to 1.7 eV (Fig. 4). However, these charges only exist under strong acidic conditions. *Via* spinless doping (see Supporting Information), we converted **PTFK** into a proof-of-concept permanent CPI (**PTFC-Ph**) (Scheme 1). Due to stabilization by resonance, **PTFC-Ph** has an even smaller band gap (1.4 eV; the polymer is green) than protonated **PTFK**. Because of the combination of soft counterions and hexyl pendant groups, **PTFC-Ph** is soluble in CH_2Cl_2, but forms hydrogels in water. Further manipulation of the pendant groups and counterions to obtain *high quality* films[7] is beyond the scope of this paper. All the absorption and

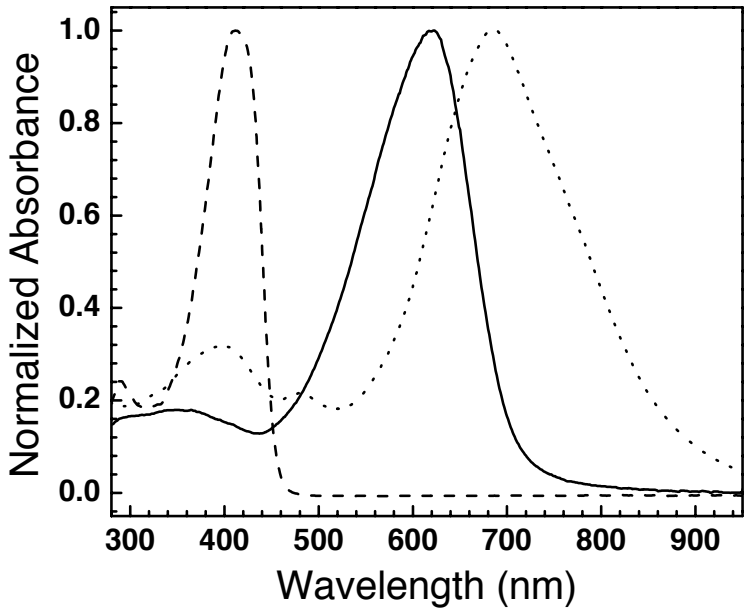

Figure 4: Normalized absorption spectrum of **PTFK** as synthesized (dashed line) and when protonated with H_2SO_4 (solid line), and **PTFC-Ph** (dotted line) in CH_2Cl_2. Protonation of the ketones results in the formation of transient carbocations and increases the conjugation length as evidenced by a large bathochromic shift. By spinless doping **PTFK** can be converted to **PTFC-Ph**–a permanent CPI–which results in a further bathochromic shift due to stabilization of the cations.

emission data are summarized in Table 1.

Table 1: Summary of optoelectronic properties of **PFK**, **PTFK**, and **PTFC-Ph**.

	λ_{max}^{abs} (nm)	λ_{max}^{ems} (nm)	Stokes Shift (nm)	E_g^{opt} (eV) [a]
PFK	340	515	175	3.3
PTFK	415	510	95	2.6
PTFK-H^+	620	–	–	1.7
PTFC-Ph	684	–	–	1.4

[a] From the band-edge tangent.

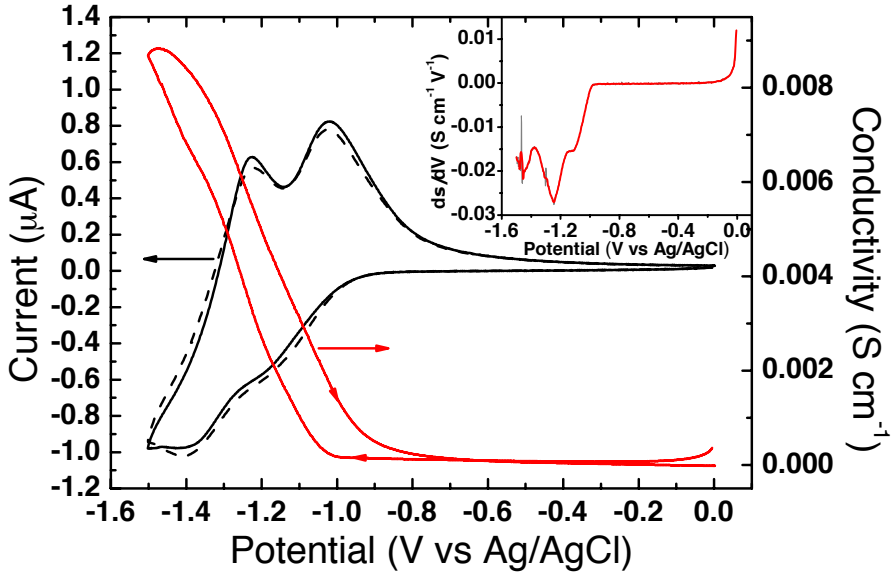

Figure 5: *In situ* conductivity measurement (red line) of **PTFK** drop-cast on interdigitated platinum electrodes scanned at 5 mV s^{-1} and 40 mV offset between the two working electrodes with 0.1 mM Bu_4NPF_6 in propylene carbonate electrolyte solution, versus Ag/AgCl. In the conductivity scan, and more clearly in its derivative (inset), multiple inflection points can be observed that we correlate to the two reduction waves, resulting in distinct charged states in the polymer. The cyclic voltammograms of the two independent working electrodes, measured at 50 mV s^{-1}, (solid and dashed black line) show negligible differences, demonstrating good coverage of **PTFK** across the electrodes.

To gain insight into the (semi)conducting properties of **PTFK** we acquired *in situ* conductivity measurements of **PTFK** drop-cast on interdigitated electrodes. As expected, we observe a fully reversible two-electron reduction (Fig. 5). The first reduction wave at −1.20 V is accompanied by a re-oxidation wave at −1.02 V and the second reduction at −1.41 V is re-oxidized at −1.23 V. As the polymer gets reduced, and the cross-conjugation broken,

the conductivity rapidly increases as radical anions are formed. The conductivity increases monotonically, but several inflection points (see inset and Fig. S6 for the derivative plot) can be recognized that coincide with the reduction waves, signifying several charged states. In linearly conjugated polymers the conductivity typically increases due to the formation of charge carriers, until a certain maximum value after which it drops rapidly again as the polymer gets doped too heavily. In **PTFK** the first reduction wave breaks the cross-conjugation and creates a radical anion. After the first wave a less conductive doubly charged state is formed, as seen by a slight change in slope. At further reduction the polymer gradually becomes doped, creating radical anions again, as seen by a second inflection point in the conductivity plot. The proposed mechanism of the formation of transient charges in **PTFK** is shown in Scheme S2. We observed similar, albeit more pronounced, doping behavior in **PTK**.[8] A plausible reason why the reduction behavior in **PTFK** appears concealed is the broad Đ and, consequently, large range of accessible states leading to gradual changes in conductivity.

To test the oxidative stability we also measured **PTFK** under positive potential (Fig. S7). We observe a (semi)reversible oxidation at $E_{1/2}$ 1.60 V but the observed shift of the oxidation peak strongly suggests (at least partial) polymer decomposition.

Device Performance

We characterized the transport of charges in **PTFK** by measuring the current-voltage (J–V) of single carrier devices. These devices were fabricated as described in the experimental section by sandwiching a polymer layer between two electrodes, chosen to suppress the injection of electrons in the conduction band (hole-only devices) or the injection of holes in the valence band (electron-only devices) of the polymer. The current flowing through such devices is space-charge limited and it depends on the mobility of charges, the applied voltage, and the thickness of the polymer layer.[34] We extracted the mobilities of electrons

and holes by fitting the experimental J–V curves with equation 1:[35]

$$J = \frac{9}{8}\epsilon_0\epsilon_r\mu_{0n(p)}\exp\left(0.891\gamma_{n(p)}\sqrt{\frac{V}{L}}\right)\frac{V^2}{L^3}\ , \tag{1}$$

where J is the current density, ϵ_0 is the permittivity of a vacuum, ϵ_r is the relative dielectric constant of the polymer, $\mu_{0n(p)}$ is the zero-field electron (hole) mobility, $\gamma_{n(p)}$ is the field activation factor, L is the thickness of the polymer layer and V is the effective voltage obtained by correcting the applied voltage V_a for the series resistance of the substrate (14 $\Omega\ \square^{-1}$ for the hole only devices, 10 $\Omega\ \square^{-1}$ for the electron only devices) and for the built-in voltage. We measured the relative dielectric constant by impedance spectroscopy, performed on a planar capacitor (Fig. S8), and we found for **PTFK** a value of 3.8, which is typical for conjugated polymers and surprisingly low given the density of polar ketone groups in the backbone.

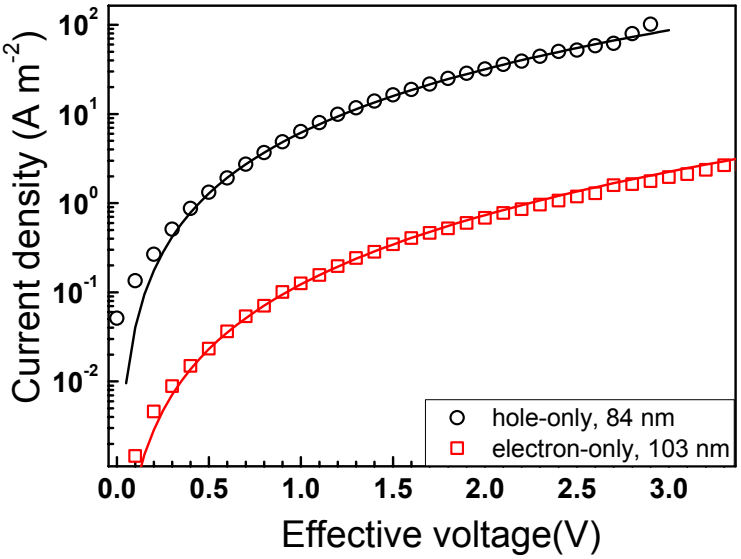

Figure 6: J–V curves of **PTFK** hole-only (black) and electron-only (red) devices. The symbols represent experimental data and the solid lines are calculated using equation 1.

The J–V characteristics of an electron-only device and of a hole-only device are displayed in Fig. 6, together with the fits (solid lines), and the fit parameters $\mu_{0n(p)}$ and $\gamma_{n(p)}$ are listed in Table 2. We found that the transport of both electrons and holes in **PTFK** are

Table 2: Fitting parameters used to plot J–V curves.

Parameter	Description	Value
μ_{0n}	Electron zero-field mobility [$cm^2\ V^{-1}\ s^{-1}$]	$1.3x10^{-8}$
γ_n	Electron field activation factor [$cm^{1/2}\ V^{-1/2}$]	$3.5x10^{-3}$
μ_{0p}	Hole zero-field mobility [$cm^2\ V^{-1}\ s^{-1}$]	$5.2x10^{-7}$
γ_p	Hole field activation factor [$cm^{1/2}\ V^{-1/2}$]	$2.0x10^{-3}$

characterized by low zero-field mobilities ($1.7x10^{-8}$—$6.6x10^{-7}$ $cm^2\ V^{-1}\ s^{-1}$) and a slight dependence on the electric field. In an attempt to improve the device characteristics, we also annealed the electron-only device above the T_g of the polymer (at 170 °C) but, unfortunately, the electron mobility actually decreased slightly (Fig. S9).

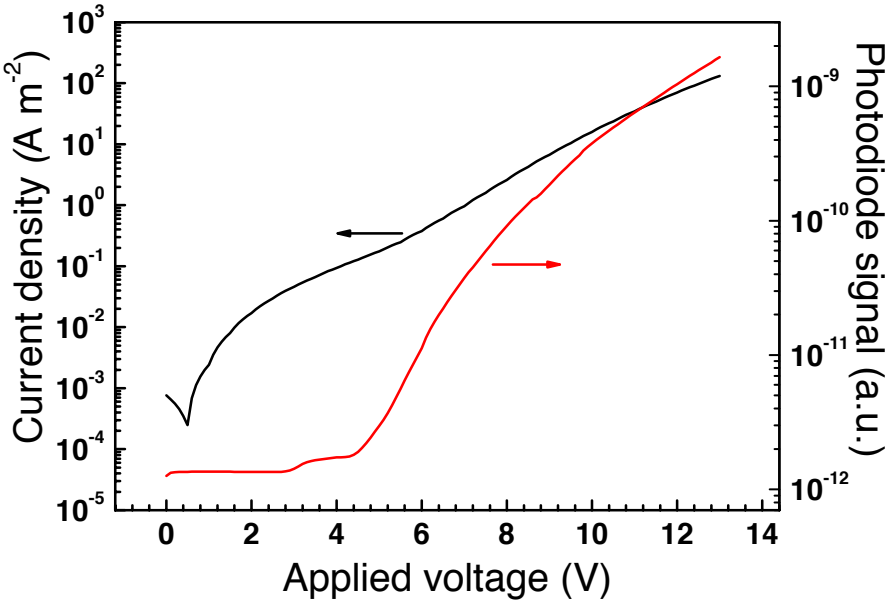

Figure 7: J–V characteristics (black) and photodiode signal (red) for a **PTFK** light emitting diode fabricated as described in the experimental section. The photodiode signal data have been smoothed by applying the adjacent average method, including 10 points per each calculation.

Fig. 7 shows the room temperature J–V characteristics of a **PTFK** light emitting diode (LED) where electrons and holes are injected in the polymer layer *via* the Ba/Al and ITO/MoO_3 contacts, respectively. We measured the light emission of the device with a silicon photodiode and plotted the photodiode signal as a function of the applied voltage as shown in Fig. 7. We then measured the emission spectrum of the light emitting diode and,

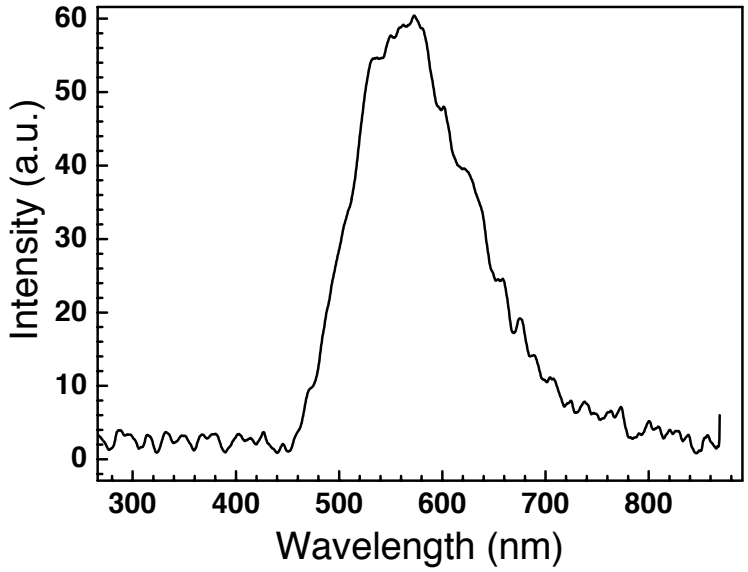

Figure 8: Emission spectrum of the **PTFK** light emitting diode.

as shown in Fig. 8, the polymer emits yellow light, with an emission peak around 570 nm. The signal measured by the silicon diode is rather weak; although holes and electrons are injected into **PTFK** and recombine radiatively, the efficiency of the LED is poor. The low mobilities and the weak emission of **PTFK** indicate non-optimal solid state packing. The full characterization of the packing parameters of **PTFK** is beyond the scope of this paper; however, the DSC data clearly show that **PTFK** is an amorphous polymer with a strong T_g and no melting temperature. This glassy nature is probably also why annealing of the electron-only device above T_g did not result in an increase in mobility. Despite the relatively poor device performance, these results demonstrate that a scalable, robust, cross-conjugated polyketone can be employed as the active material in organic devices. Further optimization may yield more useful device performances.

Conclusions

The inclusion of thiophene units in the monomer has a clear, positive effect on the polymerizability under F-C acylation polycondensation conditions. The resulting polymer, **PTFK**,

has a high degree of polymerization $P_n \sim 62$ but also a quite high dispersity $Đ \sim 5.4$. This polymer exhibits the expected properties of a CPI precursor; two-electron reduction coupled with step-wise increases in conductivity and reversible spinless doping upon protonation with a strong acid. The proof-of-concept organic LED device demonstrates that a cross-conjugated polyketone can be successfully used as an n-dopable semiconducting material, albeit with low efficiency. Nevertheless, **PTFK** is polymerized using scalable chemistry and readily accessible monomers. In combination with their excellent thermal- and oxidative stability, cross-conjugated polyketones are an interesting, new polymer platform that retains the facile optoelectronic tunability of conventional conjugated polymers. We expect that further structural optimization will eventually lead to a cross-conjugated polyketone with improved crystallinity and higher mobilities and that permanent CPIs derived from these polymers will show increased performance over their predecessors.

Experimental

Materials and Methods

All reagents and solvents were purchased from commercial sources and used without further purification unless otherwise indicated. Lewis acids were stored *in vacuo* to prevent hydrolysis and used only for a limited time. Any complexed water to the Lewis acids was removed under reduced pressure in the reaction flask at 250 °C. Terephthaloyl chloride was recrystallized from n-hexane and dried. The recrystallized terephthaloyl chloride and monomer **2** were stored *in vacuo* at 50 °C until use and purged multiple times with nitrogen in the reaction flask. All reactions were carried out under a small flow of N_2.

Monomer Synthesis

2,7-dibromo-9,9-dihexyl-9H-fluorene (1).[36] 2,7-dibromofluorene (4.86 g; 15 mmol) and Bu_4NCl (0.3 g; 1 mmol) were dissolved in DMSO (25 mL) under stirring for 30 min at rt.

50 wt% aqueous KOH (7.5 mL) was added and the solution heated to 60 °C rendering the solution deep red. To this reaction mixture 1-bromohexane (5.8 g; 35 mmol) was added and heating was continued for 24h at 60 °C after which the color steadily changed to purple. The reaction mixture was quenched by pouring it over ice H_2O (100 mL) before extracting twice with ether (2x 150 mL); the combined organic layers were washed with 10% HCl, dried over Na_2SO_4 and the solvents removed by rotary evaporation. The crude product was dissolved in $CHCl_3$ (20 mL) and purified by column chromatography on silica gel with petroleum ether as the eluent. The product was purified further by recrystallization from hexane to afford **1** as white crystals (11.132 g, 76%). ^{1}H-NMR (400 MHz, $CDCl_3$) δ 7.52 (dd, J = 7.4, 1.4 Hz, 2H), 7.45 (dd, J = 7.4, 1.5 Hz, 2H), 7.44 (d, J = 1.5 Hz, 2H), 1.99 1.84 (m, 4H), 1.18 0.99 (m, 12H), 0.78 (t, J = 7.1 Hz, 6H), 0.60 (m, 4H). ^{13}C-NMR (75 MHz, $CDCl_3$) δ 152.75, 139.26, 130.35, 126.37, 121.66, 121.34, 55.89, 40.42, 31.67, 29.79, 23.85, 22.79, 14.22. FT-IR (ATR) 3066, 2963, 2945, 2921, 2852, 1870, 1745, 1596, 1565, 1462, 1451, 1445, 1428, 1413, 1393, 1372, 1340, 1288, 1271, 1254, 1228, 1214, 1166, 1129, 1110, 1058, 1029, 1017, 1003, 981, 942, 896, 874, 843, 810, 782, 760, 745, 723, 663, 649 cm^{-1}.

2,2'-(9,9-dihexyl-9H-fluorene-2,7-diyl)dithiophene (2).[36] To a dried flask containing magnesium turnings (372 mg; 15.2 mmol) and dry THF (20 mL) was added 2-bromothiophene (2.48 g; 15.2 mmol) dropwise. After complete addition the mixture was refluxed for an additional 3 hours. In a second dried flask **1** (2.50 g; 5.08 mmol) was dissolved in dry THF (20 mL) and the solution purged with bubbling nitrogen for 1 hour. Next Pd(dppf)Cl_2 (35 mg) was added and the solution purged for an additional 30 minutes. The clear gray/brown Grignard reagent was then transferred *via* cannula to a dropping funnel and slowly added to the degassed solution containing **1**. After complete addition the reaction mixture was refluxed for 20h. Cooled down to rt the mixture was quenched by pouring it over 1N HCl/ice (250 mL) before extracting twice with CH_2Cl_2 (2x 150 mL); the combined organic layers were washed with DI H_2O (200 mL), brine (200 mL), dried over Na_2SO_4 and the solvents removed by rotary evaporation. The crude product was purified on a short silica

gel plug with petroleum ether:CH_2Cl_2 (10:1) as the eluent. The product was purified further by recrystallization from methanol:isopropanol (1:3) to afford **2** as green crystals (1.92 g, 76%). ^{1}H-NMR (400 MHz, $CDCl_3$) δ 7.68 (d, J = 7.9 Hz, 2H), 7.61 (dd, J = 7.9, 1.6 Hz, 2H), 7.56 (d, J = 1.0 Hz, 2H), 7.39 (dd, J = 3.6, 1.0 Hz, 2H), 7.30 (dd, J = 5.1, 1.0 Hz, 2H), 7.12 (dd, J = 5.1, 3.6 Hz, 2H), 2.06 – 1.97 (m, 4H), 1.17 – 0.98 (m, 12H), 0.75 (t, J = 7.0 Hz, 6H), 0.73 – 0.63 (m, 4H). ^{13}C-NMR (75 MHz, $CDCl_3$) δ 151.66, 145.14, 140.17, 133.23, 128.04, 124.95, 124.51, 122.87, 120.11, 120.06, 55.26, 40.42, 31.44, 29.65, 23.70, 22.56, 13.99.

Polymer Synthesis

Poly[(5-(9,9-dihexyl-7-(thiophen-2-yl)-9H-fluoren-2-yl)thiophen-2-yl)-*alt*-((1,4-phenylene)dimethanone)] (PTFK). $AlCl_3$ (2.758 g; 20.734 mmol) and LiCl (10 wt% of $AlCl_3$) were carefully heated at 250 °C *in vacuo* in a dried flask before adding freshly distilled 1,2–dichlorobenzene (60 mL). To a second dried flask was added **2** (3.000 g; 6.015 mmol) and freshly recrystallized terephthaloyl chloride (1.203 g; 5.924 mmol), to freshly distilled 1,2–dichlorobenzene (40 mL). The Lewis acid solution was cooled to 0 °C, the monomers solution transferred to a dropping funnel, and slowly added under vigorous stirring, resulting in a deep purple slurry. The reaction mixture was then heated at 70 °C for 20h under a flow of nitrogen (with an outflow through an alkaline scrubber). Cooled down to rt the reaction mixture was quenched by pouring it over stirring 1N HCl/ice (200 mL) before extracting four times with CH_3Cl (4x 150 mL); the combined organic layers were washed with DI H_2O (250 mL), brine (250 mL), and the solvents removed by rotary evaporation. The crude polymer was redissolved in hot THF (100 mL) and precipitated into ice-cold CH_3OH (1 L) and the precipitate collected by centrifugation at 4000 RPM for 20 min, decanting the supernatant, and drying *in vacuo* at 50 °C. The polymer was purified further *via* continuous soxhlet extraction with CH_3OH, $CH_3(CH_2)_4CH_3$, CH_3COCH_3, and $CHCl_3$. The $CHCl_3$ fraction was concentrated by rotary evaporation and the viscous solution re-precipitated (in order to obtain pellet-like particles) into ice-cold CH_3OH (1 L) and the precipitate collected

by centrifugation at 4000 RPM for 20 min, decanting the supernatant, and drying *in vacuo* at 50 °C affording **PTFK** as yellow pellets (2.87 g; 76%). ^{1}H NMR (400 MHz, CD_2Cl_2) δ 8.12 (d, J = 7.7 Hz), 8.04 (d), 7.91 (dd), 7.86 – 7.63 (m), 7.63 – 7.58 (m), 7.54 (dd), 7.44 (dd), 7.34 (dd), 7.15 (dd), 2.24 – 1.96 (m), 1.20 – 0.98 (m), 0.83 – 0.62 (m). ^{13}C-NMR (75 MHz, $CDCl_3$) δ 186.94, 154.30, 152.28, 152.02, 142.10, 141.64, 140.99, 139.72, 136.44, 133.85, 132.46, 131.87, 129.15, 128.99, 128.10, 125.54, 125.41, 124.94, 124.79, 124.11, 123.92, 123.11, 120.74, 120.69, 120.43, 120.26, 120.20, 55.61, 55.45, 40.24, 31.44, 29.55, 23.78, 22.50, 13.71. FT-IR (ATR) 3241, 3068, 2948, 2928, 2856, 2725, 1629, 1564, 1523, 1499, 1466, 1440, 1417, 1378, 1339, 1280, 1178, 1137, 1116, 1062, 1015, 981, 912, 899, 874, 849, 806, 774, 715, 694 cm^{-1}. GPC (THF) $\bar{M}_n$ = 7,250 g/mol, $\bar{M}_w$ = 38,800, $\bar{M}_p$ = 8,900 g/mol, Đ = 5.4.

Characterization

NMR spectra were measured using a Varian VXR300 (300 MHz) or a Varian AMX400 (400 MHz) instrument at 25 °C. FT-IR spectra were recorded on a Nicolet Nexus FT-IR fitted with a Thermo Scientific Smart iTR sampler. GPC measurements were done on a Spectra Physics AS 1000 series machine equipped with a Viskotek H-502 viscometer and a Shodex RI-71 refractive index detector. The columns (PLGel 5m mixed-C) (Polymer Laboratories) were calibrated using narrow disperse polystyrene standards (Polymer Laboratories). Samples were made in THF at a concentration of 3.5 mg mL^{-1} and filtered through a Gelman GHP Acrodisc 0.45 μm membrane filter before injection. Thermal properties of the polymers were determined on a TA instruments DSC Q20 and a TGA Q50. DSC measurements were executed with two heating-cooling cycles with a scan rate of 10 °C min^{-1} and from each scan the second heating cycle was selected. TGA measurements were done from 20 °C to 700 °C with a heating rate of 20 °C min^{-1}. UV/Vis measurements were carried out on a Jenway 6715 spectrometer, in 1 cm fused quartz cuvettes with concentrations of 0.02-0.1 mg mL^{-1}. Emission spectra were acquired on a Horiba Jobin Yvon FluoroLog 3-22 spectrofluorometer in 1 cm fused quartz cuvettes with concentrations of 0.2 μg mL^{-1}.

In Situ Conductivity Measurements

In Situ Conductivity Measurements were carried out with an Autolab PGSTAT100 potentiostat in a four-electrode configuration where the two (independent) working electrodes were connected to a platinum interdigitated microelectrode (IME), purchased from ABTECH Scientific, inc. (USA). The IME (1025.3-M-Pt-U) consisted of 25 pairs of 10 μm digits width, 10 μm interdigit space, and 0.3 cm length. The counter electrode was a platinum wire, and the pseudo-reference was an Ag/AgCl wire that was externally calibrated against ferrocene (Fc/Fc^+). Cyclic voltammograms were recorded at 50 mV s^{-1} and conductivity traces were measured at 5 mV s^{-1} with a 40 mV offset between the two working electrodes in a 0.1 M Bu_4NPF_6 propylene carbonate electrolyte solution. Polymer films were drop-cast at a concentration of 2.5 mg/mL on the IME and allowed to dry. An average film thickness of 200 nm was determined by AFM on scratches of four different samples.

Device Fabrication and Characterization

A light emitting diode was fabricated on glass substrate prepatterned with indium tin oxide (ITO). The substrate was thoroughly cleaned by washing with detergent solution and ultrasonication in acetone and isopropyl alcohol, and subsequent UV-ozone treatment. A 10 nm thick film of MoO_3 was thermally evaporated on the substrate. **PTFK** was spin cast from $CHCl_3$ (15 mg/ml) in N_2 atmosphere. After drying of the polymer film at room temperature, the device was finished by thermal evaporation of Ba(5 nm)/Al(100 nm). Single carrier devices were fabricated on cleaned glass substrates following the same procedure as described before. The polymer films were sandwiched between Cr(1 nm)/Au(20 nm) and Pd(20 nm)/Au(80 nm) to create hole only devices; for the fabrication of electron-only devices, Al(20 nm) and Ba(5 nm)/Al(100 nm) were selected as bottom and top contact, respectively. The device used for impedance spectroscopy was fabricated with the structure Al(20 nm)/**PTFK**/LiF(1 nm)/Al(100 nm). All the metal layers have been deposited *via* thermal evaporation. Annealing of the electron only device has been done at 170 °C for

10 minutes before evaporating the top contact. Electrical measurements of the J–V characteristics of the **PTFK** LED and single carrier devices were performed using a computer-controlled Keithley 2400 source meter in N_2 atmosphere. Electroluminescence of the LED was recorded simultaneously to J–V measurement using a Hamamatsu S1336 silicon photodiode. The emission spectrum of the LED was measured with an Ocean Optic USB2000 spectrometer. Impendance spectroscopy was conducted in the range 10 Hz 1 MHz using a Solartron 1260 impedance gain-phase analyser with an AC drive voltage of 10 mV. All the measurements were performed at room temperature in a N_2 atmosphere.

Acknowledgement

This work is part of the research program of the Foundation for Fundamental Research on Matter (FOM), which is part of the Netherlands Organization for Scientific Research (NWO). The work of D. Bartesaghi is part of the research program of the Dutch Polymer Institute (DPI), project #734. This is a publication by the FOM Focus Group 'Next Generation Organic Photovoltaics', participating in the Dutch Institute for Fundamental Energy Research (DIFFER).

Supporting Information Available

The synthesis of **PTFC-Ph**, NMR spectra, FT-IR spectra, GPC data, end-group analysis, *in situ* conductivity data, and additional device characteristics can all be found in the Supporting Information. This material is available free of charge via the Internet at `http://pubs.acs.org/`.

References

(1) Azzopardi, B.; Emmott, C. J. M.; Urbina, A.; Krebs, F. C.; Mutale, J.; Nelson, J. *Energy Environ. Sci.* **2011**, *4*, 3741–3753.

(2) Söndergaard, R.; Hösel, M.; Krebs, F. C. *J. Polym. Sci., Part B: Polym. Phys.* **2013**, *51*, 16–34.

(3) Söndergaard, R.; Helgesen, M.; Jörgensen, M.; Krebs, F. C. *Adv. Energy Mater.* **2011**, *1*, 68–71.

(4) Burke, D. J.; Lipomi, D. J. *Energy Environ. Sci.* **2013**,

(5) Hu, Z.; Zhang, K.; Huang, F.; Cao, Y. *Chem. Commun.* **2015**,

(6) Henson, Z. B.; Zalar, P.; Chen, X.; Welch, G. C.; Nguyen, T.-Q.; Bazan, G. C. *J. Mater. Chem. A* **2013**, *1*, 11117–11120.

(7) Voortman, T. P.; Chiechi, R. C. *ACS Appl. Mater. Interfaces* **2015**,

(8) Chiechi, R. C.; Sonmez, G.; Wudl, F. *Adv. Funct. Mater.* **2005**, *15*, 427–432.

(9) Voortman, T. P.; de Gier, H. D.; Havenith, R. W. A.; Chiechi, R. C. *J. Mater. Chem. C* **2014**, *2*, 3407–3415.

(10) Swager, T. M.; Grubbs, R. H. *J. Am. Chem. Soc.* **1987**, *109*, 894–896.

(11) Pranata, J.; Dougherty, D. A. *Synth. Met.* **1987**, *22*, 171–178.

(12) Sonar, P.; Zhang, J.; Grimsdale, A. C.; Mllen, K.; Surin, M.; Lazzaroni, R.; Leclre, P.; Tierney, S.; Heeney, M.; McCulloch, I. *Macromolecules* **2004**, *37*, 709–715.

(13) Heeney, M.; Bailey, C.; Genevicius, K.; Shkunov, M.; Sparrowe, D.; Tierney, S.; McCulloch, I. *J. Am. Chem. Soc.* **2005**, *127*, 1078–1079.

(14) McCulloch, I. et al. *Adv. Mater.* **2009**, *21*, 1091–1109.

(15) Mike, J. F.; Nalwa, K.; Makowski, A. J.; Putnam, D.; Tomlinson, A. L.; Chaudhary, S.; Jeffries-EL, M. *Phys. Chem. Chem. Phys.* **2011**, *13*, 1338–1344.

(16) Głwacki, E. D.; Apaydin, D. H.; Bozkurt, Z.; Monkowius, U.; Demirak, K.; Tordin, E.; Himmelsbach, M.; Schwarzinger, C.; Burian, M.; Lechner, R. T.; Demitri, N.; Voss, G.; Sariciftci, N. S. *J. Mater. Chem. C* **2014**, *2*, 8089–8097.

(17) Hudson, L. G.; Stevens, M. P. *J. Polym. Sci. A Polym. Chem.* **1995**, *33*, 71–78.

(18) McClain, M. D.; Whittington, D. A.; Mitchell, D. J.; Curtis, M. D. *J. Am. Chem. Soc.* **1995**, *117*, 3887–3888.

(19) Curtis, M. D.; McClain, M. D. *Chem. Mater.* **1996**, *8*, 945–951.

(20) Goodman, I.; McIntryre, J. E.; Russell, W. Verfahren zur Herstellung polymerer Ketone. 1964; GB971227 (A).

(21) Kutz, M. *Applied Plastics Engineering Handbook: Processing and Materials*; William Andrew, 2011.

(22) Deeter, G. A.; Moore, J. S. *Macromolecules* **1993**, *26*, 2535–2541.

(23) Wang, F.; Roovers, J. *Macromolecules* **1993**, *26*, 5295–5302.

(24) Yang, J.; Tyberg, C. S.; Gibson, H. W. *Macromolecules* **1999**, *32*, 8259–8268.

(25) Milam, J.; Dean, W.; Gerdes, R. Separation of dichlorobenzene isomers. 1978; US Patent 4,089,909.

(26) Liu, B.; Dishari, S. *Chem. Eur. J.* **2008**, *14*, 7366–7375.

(27) Wang, Q.; Qu, Y.; Tian, H.; Geng, Y.; Wang, F. *Macromolecules* **2011**, *44*, 1256–1260.

(28) Nunes, R. W.; Martin, J. R.; Johnson, J. F. *Polym. Eng. Sci.* **1982**, *22*, 205–228.

(29) Savagatrup, S.; Makaram, A. S.; Burke, D. J.; Lipomi, D. J. *Adv. Funct. Mater.* **2014**, *24*, 1169–1181.

(30) Clendinning, R. A.; Kelsey, D. R.; Botkin, J. H.; Winslow, P. A.; Youssefi, M.; Cotter, R. J.; Matzner, M.; Kwiatkowski, G. T. *Macromolecules* **1993**, *26*, 2361–2365.

(31) Adger, B. Chemical process. 1987; US Patent 4,677,228.

(32) Gay, F. P.; Brunette, C. M. Ordered polyetherketones. 1989; US Patent 4,816,556.

(33) Fox, T. G. J.; Flory, P. J. *J. Appl. Phys.* **1950**, *21*, 581–591.

(34) Lampert, M. A.; Mark, P. *Current injection in solids*; Academic Press, 1970.

(35) Murgatroyd, P. N. *J. Phys. D: Appl. Phys.* **1970**, *3*, 151.

(36) Brouwer, F.; Alma, J.; Valkenier, H.; Voortman, T. P.; Hillebrand, J.; Chiechi, R. C.; Hummelen, J. C. *J. Mater. Chem.* **2011**, *21*, 1582–1592.

Graphical TOC Entry